



Cite this: *Green Chem.*, 2023, **25**, 3660

# Feedstock-agnostic reductive catalytic fractionation in alcohol and alcohol–water mixtures†

Jun Hee Jang,<sup>‡a</sup> Ana Rita C. Morais,<sup>ID ‡a</sup> Megan Browning,<sup>a</sup> David G. Brandner,<sup>ID a</sup> Jacob K. Kenny,<sup>a,b</sup> Lisa M. Stanley,<sup>a</sup> Renee M. Happs,<sup>ID a</sup> Anjaneya S. Kovvali,<sup>c,d</sup> Joshua I. Cutler,<sup>e</sup> Yuriy Román-Leshkov,<sup>ID \*f</sup> James R. Bielenberg<sup>\*d</sup> and Gregg T. Beckham<sup>ID \*a</sup>

Many biomass conversion technologies focus primarily on tailor-made processing conditions for a single feedstock, in contrast to developing a practical operational window for effective processing of a broad variety of lignocellulosic biomass substrates available year-round. Here, we demonstrate the feedstock flexibility of reductive catalytic fractionation (RCF), performed in both batch and flow-through (FT) modes, to effectively process a range of biomass types (hardwoods, softwoods, and herbaceous monocots), regardless of their macromolecular composition and morphological structure differences. Both batch and FT-RCF performed with pure methanol as a solvent allow delignification (or lignin oil yield) values and lignin monomer yields greater than 65 wt% and 25 wt%, respectively, and high retention of carbohydrates (>90%) from herbaceous monocots (corn stover and switchgrass) and hardwood (poplar) biomass substrates, despite the inherent differences between woody and herbaceous biomass feedstocks. FT-RCF of pine (softwood) exhibited lower lignin extraction efficiency (<40%), but the high content of lignin in pine enabled a similar lignin oil yield on a biomass basis relative to other feedstocks. FT-RCF was subsequently tested by adding water as a co-solvent (*i.e.*, 50 : 50 w/w methanol/water), and delignification values increased to greater than 78% regardless of the feedstock. Together with the comparable delignification values, similar lignin oil and carbohydrate yields, as well as lignin oil properties, were observed across the tested feedstocks, suggesting that RCF with an alcohol/water mixture can effectively and consistently handle a wide range of lignocellulosic biomasses, including hardwoods, softwood, and herbaceous biomasses.

Received 24th November 2022,  
Accepted 6th April 2023

DOI: 10.1039/d2gc04464a

[rsc.li/greenchem](http://rsc.li/greenchem)

## Introduction

The longstanding interest in developing a large-scale bioeconomy has driven the need for a highly available, consistent, and stable supply of biomass feedstocks for producing bio-based fuels and chemicals.<sup>1</sup> However, many places in the world do

not have access to a single low-cost biomass feedstock with the year-round availability necessary to meet the high feedstock capacity necessary for economically feasible biorefinery operations. The viability of bio-based fuels and chemicals will partially depend on the development of robust biomass processing technologies that can effectively handle biomass variability regarding particle morphology, intra-particle pore structure, and biomass structure and composition.<sup>2</sup> These properties are dependent on biomass type, growing conditions, harvesting, handling, and storage.<sup>3,4</sup> Research of leading biomass conversion technologies, such as those using mineral acids, steam explosion, or ammonia-fiber expansion (AFEX<sup>TM</sup>), often focus primarily on tailor-made processing conditions for a single feedstock, and thus the developed processing conditions may not be applicable to different types of biomass substrates.<sup>5</sup> For example, while dilute-acid hydrolysis and AFEX<sup>TM</sup> are effective in processing agricultural residues like corn stover and wheat straw, they are unable to economically process hardwoods.<sup>5,6</sup> Significant efforts have therefore been made towards the development of feedstock-agnostic techno-

<sup>a</sup>Renewable Resources and Enabling Sciences Center, National Renewable Energy Laboratory, Golden, CO 80401, USA. E-mail: [gregg.beckham@nrel.gov](mailto:gregg.beckham@nrel.gov)

<sup>b</sup>Department of Chemical and Biological Engineering, University of Colorado Boulder, Boulder, CO 80303, USA

<sup>c</sup>Office of Clean Energy Demonstrations, U.S. Department of Energy, Washington, DC 20585, USA

<sup>d</sup>ExxonMobil Research and Engineering, Clinton, NJ 08809, USA. E-mail: [james.bielenberg@exxonmobil.com](mailto:james.bielenberg@exxonmobil.com)

<sup>e</sup>ExxonMobil Chemical Company, Baytown, TX 77520, USA

<sup>f</sup>Department of Chemical Engineering, Massachusetts Institute of Technology, Cambridge, MA 02139, USA. E-mail: [yroman@mit.edu](mailto:yroman@mit.edu)

†Electronic supplementary information (ESI) available. See DOI: <https://doi.org/10.1039/d2gc04464a>

‡Co-first author.



logies that can be applied to a variety of biomasses, independently of their type, composition, and structural morphology. For example, thermochemical processes such as pyrolysis and gasification are more robust to feedstock type,<sup>7</sup> and the use of ionic liquids (ILs) affords fractionation for hardwoods, softwoods, herbaceous dicots, and monocots.<sup>8–10</sup>

Additionally, a new class of biomass conversion technologies based on tandem biomass fractionation and lignin depolymerization/stabilization, which is termed lignin-first biorefining, has been developed to avoid lignin degradation by either the use of heterogeneous reducing catalysts or chemical stabilization agents to stabilize reactive intermediates.<sup>11–17</sup> Of note among lignin-first biorefining methods, reductive catalytic fractionation (RCF) is an active stabilization technology capable of producing depolymerized lignin oil while preserving the biomass carbohydrates.<sup>17</sup> Specifically, RCF involves solvent-mediated extraction of lignin fragments from biomass, followed by the depolymerization and stabilization of reactive lignin-derived intermediates over a redox-active catalyst through hydrogenolysis and hydrogenation reactions in the presence of H<sub>2</sub> or a hydrogen donor.<sup>18,19</sup> The outcome of the RCF process is lignin oil composed of a narrow distribution of monomers in near-theoretical yields along with dimers and low molecular weight oligomers, as well as a carbohydrate-rich pulp.<sup>17,20</sup> The composition of the solid pulp from RCF typically includes cellulose with varying quantities of hemicelluloses and residual lignin, which depend on the reaction conditions.<sup>17</sup> To achieve an economically viable RCF process,<sup>21</sup> reactor configurations,<sup>22–25</sup> low-pressure solvent systems,<sup>26</sup> solvent recycling,<sup>27,28</sup> catalyst type,<sup>29,30</sup> and utilization of entire RCF oil,<sup>31</sup> have been pursued. Along with these process innovations, RCF has been applied to hardwoods (poplar,<sup>32</sup> oak,<sup>33</sup> beech,<sup>34</sup> and eucalyptus<sup>20</sup>), softwoods (pine<sup>35</sup> and spruce<sup>36</sup>), and herbaceous biomasses (corn stover,<sup>18</sup> switchgrass,<sup>37</sup> *Miscanthus × giganteus*,<sup>38</sup> walnut shell,<sup>39</sup> and wheat straw<sup>40</sup>). In reports to date, RCF has been shown to be applicable to a wide range of feedstocks, suggesting the potential for this process technology to be feedstock agnostic.

In the present work, RCF was applied to poplar (hardwood), switchgrass (herbaceous monocot), corn stover (herbaceous monocot), and pine (softwood), in batch RCF conditions, at varying solvent compositions (alcohol and alcohol/water), to first provide insights into the conditions required to maximize lignin extraction and depolymerization for each feedstock. Subsequently, RCF was performed on each feedstock using a flow-through (FT) reactor,<sup>19,22,23</sup> to determine the effect of biomass type on lignin extraction, monomer yield, and carbohydrate recovery. By studying the impact of feedstock type on RCF performance, this work intends to provide a technical assessment regarding the feasibility of RCF to be used as a feedstock-agnostic technology.

## Experimental section

### Chemicals

Ethanol (≥99.6%), methanol (≥99.8%), and ethyl acetate (≥99.5%) were purchased from Fischer Scientific. Sulfuric acid

(72 wt%) was purchased from Macron. Acetone-d<sub>6</sub> (99.9 atom% D), dimethyl sulfoxide-d<sub>6</sub> (99.9 atom% D), pyridine (anhydrous, 99.8%), acetic anhydride (99.5%), tetrahydrofuran (inhibitor-free, ≥99.9%), 1,3,5-tri-*tert*-butylbenzene (97%), ruthenium on carbon (Ru/C, 5 wt%), coarse fused silica (4–20 mesh), and glass beads (5 mm) were purchased from Sigma-Aldrich. Borosilicate glass wool was purchased from the Ohio Valley Specialty Company. Fine fused silica (30/50 grade) was purchased from Dupre Minerals.

### Biomass substrates

The four feedstocks included in this study were poplar, switchgrass, corn stover, and pine. Hybrid poplar was harvested in Morrow County, OR in 2013 and provided by Greenwood Resources. Switchgrass was harvested at in Garvin County, OK in 2012 and provided by Oklahoma State University. Corn stover was harvested in Boone, IA and provided by Idaho National Laboratory. Pine was harvested in Edgefield, SC and provided by FTX Consulting. All biomasses were size reduced *via* knife-milling (Thomas Scientific Wiley Mill) through a 2 mm screen and stored at room temperature in closed containers until use.<sup>41</sup> Compositional analyses were performed based on a standard compositional analysis using NREL's Laboratory Analytical Procedure described elsewhere.<sup>42–44</sup> Table S1† contains the compositions of the biomass substrates.

### Batch reductive catalytic fractionation

RCF batch experiments were conducted in a magnetically-stirred reactor (Parr, 5000 series, 75 mL). The reactors were filled with 2 g of (non-dried) feedstock, 30 mL of solvent, and 400 mg of 5 wt% Ru/C. The reactors were closed and purged with high pressure He (three cycles), then pressurized with 30 bar of H<sub>2</sub>. Subsequently, the reactors were heated to 230 °C (heating time of 30 min). The operating pressure reached 80–83 and 65–70 bar with methanol and methanol/water, respectively, at 230 °C. The reaction time was started once the reactors reached the set temperature. After 4 h of residence time, the reactors were quenched in cold water and depressurized at room temperature. The reaction slurry was filtered using a 0.2 µm filter.

### Flow-through reductive catalytic fractionation

FT reactions were performed using a custom-built flow reactor with two biomass beds (5/8" ID) and one catalyst bed (9/32" ID). The experimental equipment and procedures have been previously described in detail.<sup>19,22,28</sup> In the FT-RCF experiments, each biomass bed was packed with 2.7 g of (non-dried) biomass and the catalyst bed (downstream of the biomass) was packed with 0.9 g of 5 wt% Ru/C, diluted with 2.1 g of fine fused silica. Solvent and hydrogen flow rates were 2 mL min<sup>−1</sup> and 200 SCCM, respectively. The first biomass and catalyst bed were run in series at 1600 psig (110 bar) of total pressure for a 1 h heating ramp and 3 h reaction time at 225 °C. Duplicates were performed with the second biomass bed, maintaining the same catalyst bed. Liquid samples were collected and ana-



lyzed for monomer yield and lignin oil properties. The pulp residue from the biomass beds was used for compositional analysis.

### Lignin oil analysis

Lignin oils from batch and FT-RCF were obtained by evaporating the solvent and performing liquid–liquid extraction. After removing the solvent using rotary evaporation, the resulting oil underwent liquid–liquid extraction with 10 mL of DI water and ethyl acetate. The water fraction was extracted again with 5 mL of ethyl acetate (3 cycles). Sodium sulfate was added to the ethyl acetate fraction to remove residual water. The ethyl acetate fraction was dried and weighed to obtain the lignin oil yield. The lignin oil yields were calculated on a weight basis using the following equation:

$$\text{Oilyield (\%)} = \frac{\text{mass}_{\text{lignin oil}}}{\text{mass}_{\text{feedstock, initial}} \times \text{initial lignin content}} \times 100 \quad (1)$$

### Gas chromatography (GC) analysis

Lignin-derived monomers were quantified using an Agilent GC (8890 series) equipped with a HP5-column and a flame ionization detector (FID) was used to analyze the samples. GC samples were prepared by diluting a liquid sample aliquot with methanol containing 1,3,5-tri-*tert*-butylbenzene as an internal standard. The operation conditions were as follows: injection temperature of 250 °C; column temperature program: 70 °C, 2 min hold, 10 °C min<sup>−1</sup> to 280 °C, 2 min hold; detection temperature of 300 °C. The monomer yields were calculated on a weight basis using the following equation:

$$\text{Monomeryield (\%)} = \frac{\text{mass}_{\text{monomer}}}{\text{mass}_{\text{feedstock, initial}} \times \text{initial lignin content}} \times 100 \quad (2)$$

### Gel permeation chromatography (GPC)

Lignin oil molecular weight distributions of post FT-RCF reactions were determined using GPC as described previously.<sup>41</sup> Briefly, approximately 20 mg of the isolated oil sample was acetylated with 1 mL of 50 : 50 v/v mixture of acetic anhydride and pyridine at 40 °C for 24 h with stirring. Subsequently, 1 mL of methanol was added to terminate the reaction, and the reagents were removed by evaporation under flowing nitrogen. The addition-drying step with methanol was repeated five times. Acetylated samples were dried in a vacuum oven (~0.7 bar) at 40 °C overnight, dissolved in tetrahydrofuran, and filtered through a 0.2 µm filter. For the GPC measurements, 20 µL of each prepared sample was injected on a high-performance liquid chromatography (HPLC) installed with PLgel 7.5 × 300 mm columns: 10 µm × 50 Å, 10 µm × 103 Å, 10 µm × 104 Å (Agilent Technologies). The measurement was conducted at ambient temperature by flowing isocratic tetrahydrofuran (1 mL min<sup>−1</sup>) for 40 min, with measurements taken at 210 nm, 260 nm, and 270 nm on the diode array detector.

### Heteronuclear single-quantum coherence (HSQC) 2D-NMR spectroscopy

To prepare an NMR sample, 20 mg of the post-extraction lignin oil was dissolved in 700 µL acetone-d<sub>6</sub>. HSQC NMR spectra were acquired in a 11.7 T (600 MHz) Bruker Avance III spectrometer with a room temperature broadband probe. For spectra, 1024 points for an acquisition time (AQ) of 71 ms and a spectral width (SW) of 12 ppm were acquired in the F2 (<sup>1</sup>H) dimension and 256 points for an AQ of 1.93 ms and a SW of 220 ppm were used in the F1 (<sup>13</sup>C) dimension with a standard phase-sensitive, gradient-selected pulse sequence. The acquired spectra were processed using TopSpin 4.1.4 with previously reported spectral processing parameters.<sup>45</sup>

### Carbohydrate pulp characterization

Carbohydrate pulps from RCF were subjected to a standard compositional analysis protocol.<sup>43</sup> Briefly, the post-reaction carbohydrate pulp was dried and subjected to acid hydrolysis (72 wt% sulfuric acid) at 30 °C for 1 h. Then, the suspension was diluted to a 4% acid concentration and autoclaved at 121 °C for 1 h, followed by filtration to yield the Klason lignin (acid-insoluble lignin). The acid-soluble lignin was quantified *via* absorbance measurements at 240 nm wavelength. The carbohydrate fraction was quantified using HPLC with a Shodex Sugar SP0810 column coupled with a de-ashing guard-column (Bio-Rad No. 1250118). We note that the concentration of polymeric sugars (glucan, xylan, galactan, arabinan, and mannan) was calculated from the concentration of the corresponding monomeric sugars.<sup>43</sup> Thus, glucan was calculated based on glucose from cellulose and hemicellulose fractions. Delignification and retention of glucan/xylan were calculated using the following equations:

$$\text{Delignification (\%)} = \left( 1 - \frac{\text{mass}_{\text{lignin in pulp sample}}}{\text{mass}_{\text{initial loaded lignin}}} \right) \times 100 \quad (3)$$

$$\text{Glucan retention (\%)} = \left( \frac{\text{mass}_{\text{glucan in pulp sample}}}{\text{mass}_{\text{initial loaded glucan}}} \right) \times 100 \quad (4)$$

$$\text{Xylan retention (\%)} = \left( \frac{\text{mass}_{\text{xylan in pulp sample}}}{\text{mass}_{\text{initial loaded xylan}}} \right) \times 100 \quad (5)$$

## Results

### Batch RCF of woody and herbaceous biomasses

RCF was first conducted on poplar, switchgrass, corn stover, and pine with four solvent systems in batch reactors to investigate the effect of biomass types and composition on process performance for simultaneous extraction of lignin and production of aromatic monomers. Methanol is a commonly used solvent in RCF reactions to extract and depolymerize lignin while retaining carbohydrates.<sup>46–48</sup> In addition, ethanol has been frequently used in RCF due to its availability from cellulosic ethanol production.<sup>47,49,50</sup> Alcohol/water mixtures have also been used as RCF solvents, exhibiting higher delignifica-





### Flow-through RCF of woody and herbaceous lignin

FT-RCF is a semi-batch type reaction wherein the biomass and catalyst are located in separate beds and the solvent flows over the biomass and catalyst beds in series for tandem lignin extraction and reductive stabilization. This setup enables physical separation and recovery of the catalyst and carbohydrate-rich pulp, which is a challenge for batch RCF operation.<sup>19,22,23,25,55–57</sup> To evaluate the fractionation efficiency and monomer yields through RCF with different types of feedstocks, we conducted FT-RCF reactions with methanol and 50 : 50 w/w methanol/water. Subsequently, the produced lignin oil and solid pulp residue were analyzed. We note that FT-RCF is an experimentally convenient construct, but acknowledge that processes would likely not be run in these conditions at scale due to overly high solvent usage (180 L solvent per kg biomass) in single-pass FT-RCF mode.

### Fractionation efficiency

Each native feedstock has a unique composition (Fig. 2A). The compositions of as-received and dried feedstocks are shown in Table S1†. All results are calculated on a dry weight basis unless otherwise noted. Concerning lignin, poplar contains 26% lignin whereas switchgrass and corn stover have 17–18% lignin content. Pine showed the highest lignin percentage of 34%. Glucan and xylan are the major carbohydrates in native poplar, switchgrass, and corn stover. For pine, mannan (11%), not xylan (7%) is the dominant polysaccharide in its hemicellulosic fraction.

After the FT-RCF reactions, changes in composition of biomass could estimate the extent of lignin removal and carbohydrate retention (Fig. 2B). FT-RCF of poplar in methanol selectively extracted lignin ( $64.0 \pm 0.2\%$ ) with high glucan and xylan retention ( $98.4 \pm 0.2\%$  and  $101.4 \pm 0.8\%$ , respectively). In agreement with the batch reaction results, the use of a 50 : 50 w/w methanol/water solvent system significantly increased

delignification to  $92.5 \pm 0.7\%$  relative to pure methanol. However, xylan retention decreased significantly with the addition of water as a co-solvent to  $15.2 \pm 0.03\%$ , while glucan retention remained high ( $86.1 \pm 1.1\%$ ).<sup>58</sup> In previous studies, it was reported that the extracted hemicellulose dissolved in water is likely depolymerized into oligomeric sugars, monomeric C5–C6 sugars, and C2–C6 polyols.<sup>20,50</sup>

RCF of switchgrass and corn stover showed similar fractionation efficiency to that of poplar. Delignification values obtained from methanol RCF ( $64.6 \pm 0.6\%$  and  $70.9 \pm 0.6\%$  for switchgrass and corn stover, respectively) increased to 94.5 and 92.5% in RCF with a methanol/water mixture. Although xylan retention values in methanol RCF (93–100%) were significantly reduced to 17–22% in methanol/water RCF, glucan retention remained high (>88%) regardless of solvent. RCF of pine with methanol exhibited lower delignification of  $32.9 \pm 0.9\%$  relative to the three other feedstocks. Methanol/water RCF increased the delignification extent to  $77.9 \pm 1.2\%$ , which enables consideration of pine as a candidate for feedstock-agnostic processes with hardwoods and herbaceous biomasses.

### Lignin oil and monomers

To characterize the lignin oil and monomers and measure their yields, liquid samples underwent solvent removal, followed by liquid–liquid extraction, thus isolating the lignin oil from the RCF oil (Fig. 3 and Table S3†). In the literature, oil yield has been used to estimate the extent of lignin extraction,<sup>18,47</sup> but discrepancies between oil yield and delignification could be observed because liquid–liquid extraction may not selectively isolate only lignin from the RCF oil. In particular, extractives and acetates (Fig. 2A) extracted from biomass by the solvent likely remain in the organic ethyl acetate phase during liquid–liquid extraction and cause an overestimation of the oil yield.<sup>17</sup> A high extractives (8–9%,

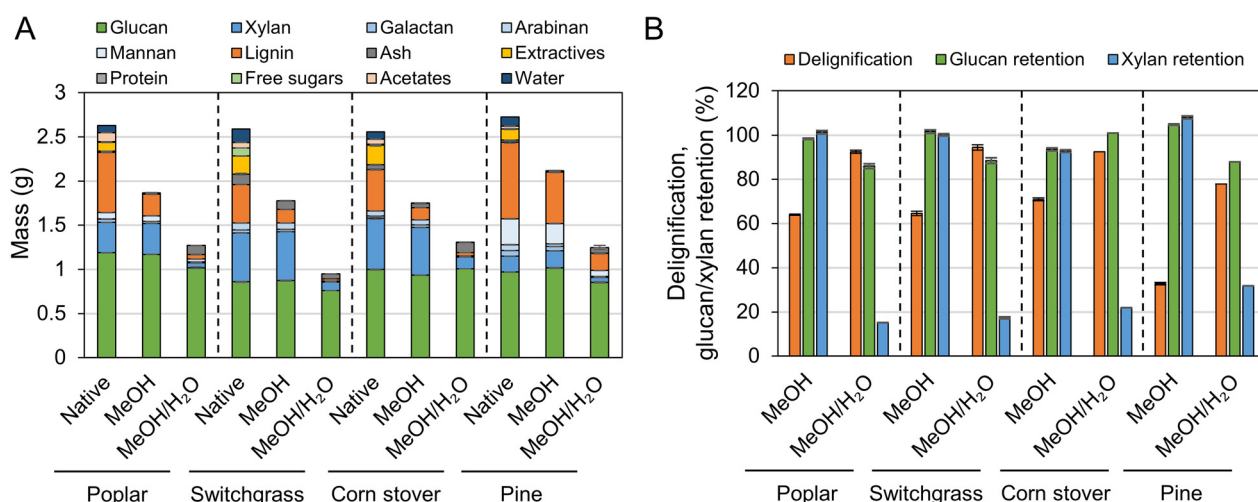


**Fig. 2** FT-RCF with poplar, switchgrass, corn stover, and pine in methanol or methanol/water mixture. (A) Compositional analysis of native feedstocks and post-RCF carbohydrate-rich pulps. (B) Calculated delignification and glucan and xylan retention. FT-RCF reaction conditions:  $2 \text{ mL min}^{-1}$  feed solvent, 2.7 g feedstock, 0.9 g 5 wt% Ru/C (diluted with 2.1 g of fused silica), 1600 psig (110 bar), 200 SCCM H<sub>2</sub>, 225 °C, and 1 h heating ramp and 3 h run. Table S1† contains the quantitative information for the data shown here. The error bars are the range of duplicates.



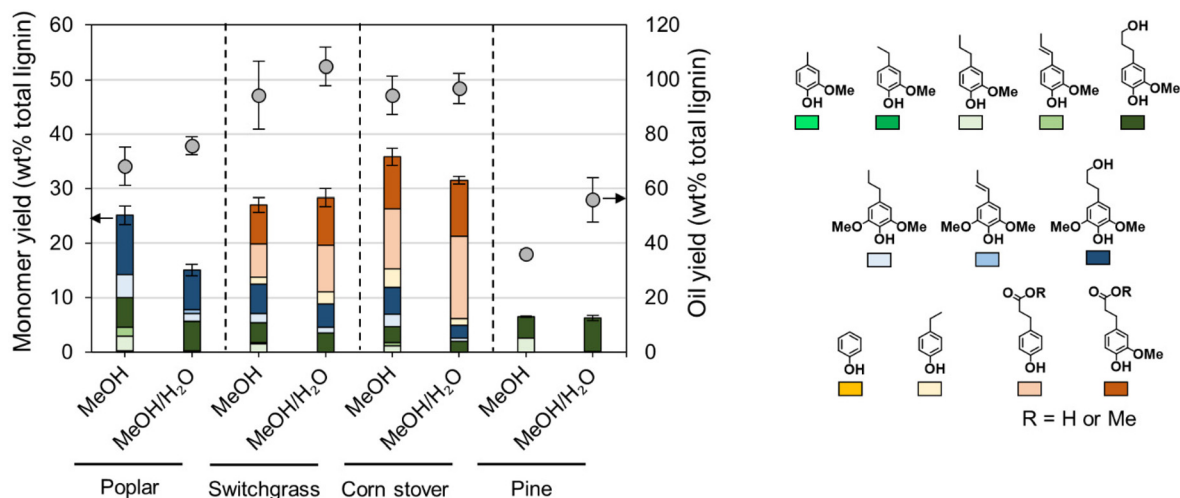


**Fig. 3** Monomer and oil yields of FT-RCF with poplar, switchgrass, corn stover, and pine in methanol or methanol/water mixture. Reaction conditions: 2 mL min<sup>-1</sup> feed solvent, 2.7 g feedstock, 0.9 g 5 wt% Ru/C (diluted with 2.1 g of fused silica), 1600 psig (110 bar), 200 SCCM H<sub>2</sub>, 225 °C, and 1 h heating ramp and 3 h run. Table S3† contains the quantitative information for the data shown here. The error bars are the range of total monomer yields and oil yields of duplicates.

Fig. 2A) and acetates (2–3%) content, coupled with low lignin content (17–18%) in switchgrass and corn stover would therefore result in the significant overestimation of oil yield, and indeed, methanol RCF of switchgrass and corn stover exhibited higher lignin oil yields (88.9 ± 12.4% and 94.2 ± 7.0%, respectively) than their delignification values (64.6 ± 0.6% and 70.9 ± 0.6%, respectively). We note that extractives such as fatty acids could be co-processed with lignin oil, for example through hydrodeoxygenation processes.<sup>59</sup> Compared to herbaceous biomass types, poplar and pine exhibited higher lignin contents (26% and 34%, respectively) and lower amounts of extractives (4–5%), reducing the effect of extractives and acetates on the measured oil yields. We note that the water content was negligible (0.4–0.6 wt%) in lignin oils from RCF of corn stover and switchgrass in methanol/water.

Conversely, in methanol/water RCF of poplar, the oil yield (75.7 ± 3.2%) was lower than the delignification extent of 92.5

± 0.7%. The lower oil yield relative to the delignification arose because (1) lignin is partially deoxygenated during the depolymerization process and (2) some portion of the lignin extracted from biomass and included in RCF oil was not collected in the organic phase, but remained in the aqueous phase during liquid–liquid extraction. This is supported by the mass flow of the major biomass components (Fig. 4), UV-Vis (Fig. S7†), and HSQC 2D NMR (Fig. S8†) analyses of the aqueous phase. During methanol/water RCF of poplar, the extracted lignin (24.1 wt%) of total lignin (26.0 wt%) remained in RCF oil (54.0 wt%). However, liquid–liquid extraction of the RCF oil produced only 19.6 wt% lignin oil, suggesting incomplete recovery of lignin in the extraction step. UV-Vis analysis revealed that the aqueous phase contained 3.8 g L<sup>-1</sup> lignin (8.1 wt% of the initial lignin), supporting the contention of lignin loss during extraction and the resulting lower lignin oil yield than the measured delignification extent (Fig. S7†).

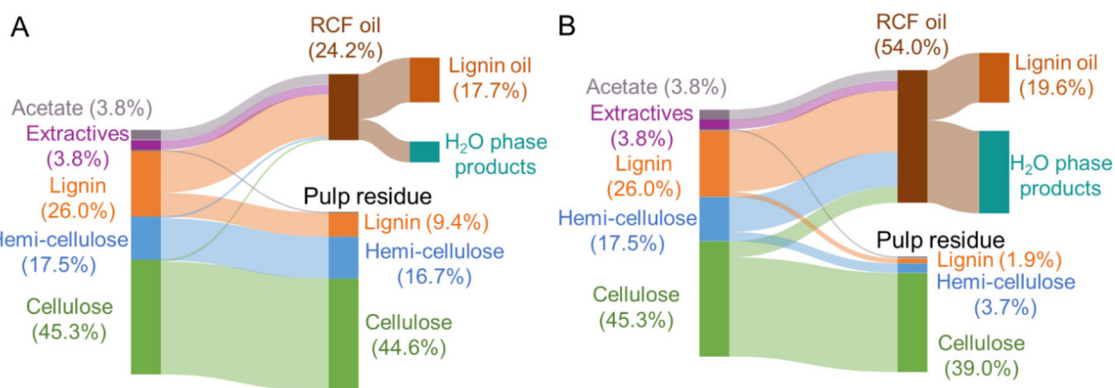


**Fig. 4** Mass flow of major components of biomass (A) FT-RCF of poplar in methanol. (B) FT-RCF of poplar in methanol/water. RCF oil represents the oil after solvent removal of liquid RCF samples. Lignin oil is the oil obtained from the organic phase after liquid–liquid extraction of the RCF oil.

Consistently, *p*-hydroxybenzoic acid or methylparaben peaks were detected in the HSQC spectra of solid products dissolved in the aqueous phase (Fig. S8†). It is worth noting that only 1.8 wt% of the initial lignin was detected in the aqueous phase obtained from methanol RCF of poplar and subsequent liquid–liquid extraction. In methanol/water RCF of switchgrass and corn stover, the opposite effects of extractives and acetates and lignin loss during extraction seem to be reflected in the lignin oil yields (96–105%), which were close to the delignification values (92–95%).

The lignin monomers collected at different times during the FT-RCF reactions were also analyzed by GC-FID. The cumulative monomer yields over the 3 h reaction are shown in Fig. 3 and Fig. S9, Table S3.† In poplar-RCF with methanol, the cumulative monomer yield for the first biomass bed was 26.3% which was slightly lower than the monomer yield in a batch reactor ( $32.6 \pm 2.7\%$ ) even with a similar lignin oil yield ( $65.1 \pm 8.7\%$  in batch and  $68.2 \pm 7.0\%$  in FT). The second biomass bed with a reused catalyst bed showed a 24.0% cumulative monomer yield, indicative of catalyst deactivation. In the same reactor system, we previously observed a decrease in the monomer yield (from 22% to 16%) and increase in the selectivity of unsaturated monomers (from 2% to 18%) over the consecutive FT-RCF reactions with 6 biomass beds while reusing the catalyst.<sup>28</sup> Catalyst deactivation likely arose due to sintering, leaching, and poisoning, as observed in our previous

study.<sup>22</sup> The average cumulative monomer yield of two FT-RCF reactions was  $25.2 \pm 1.7\%$ . Arylpropanol lignin monomers were dominant, whereas the batch reactions produced arylpropyl monomers as the major products. Note the distribution of stabilized lignin monomers from FT-RCF did not change even with additional batch or FT catalysis steps, excluding the effect of catalytic residence time on monomer selectivity.<sup>28</sup>

The lignin oil was also analyzed by GPC and HSQC 2D NMR (Fig. 5 and Fig. S10†). In the GPC trace of the poplar lignin oil from FT-RCF with methanol, peaks at 200 and 250 Da are assigned to propyl- and propanol-substituted monomers.<sup>15,18,22,28,47</sup> The larger molecular weight peaks at 310, 540, and 750 likely represent the dimer, trimer, and tetramer peaks, respectively. NMR analysis of the lignin oil supports depolymerization of lignin during FT-RCF by showing the disappearance of  $\beta$ -ether units and the appearance of propanol and propyl sidechain peaks (Fig. 5B and Fig. S10A†).

Whereas the use of a 50 : 50 w/w methanol/water mixture instead of pure methanol increased delignification to 92.5%, the cumulative monomer yield was reduced to  $15.0 \pm 1.1\%$ . Consistently, the significant reduction of monomer peaks at 200 and 250 Da was observed in the GPC trace of the lignin oil from FT-RCF reaction in methanol/water. The higher portion of oligomers, compared to that from methanol RCF, suggests either that depolymerization was not effective or condensation occurred in the presence of water. The absence of  $\beta$ -O-4 lin-

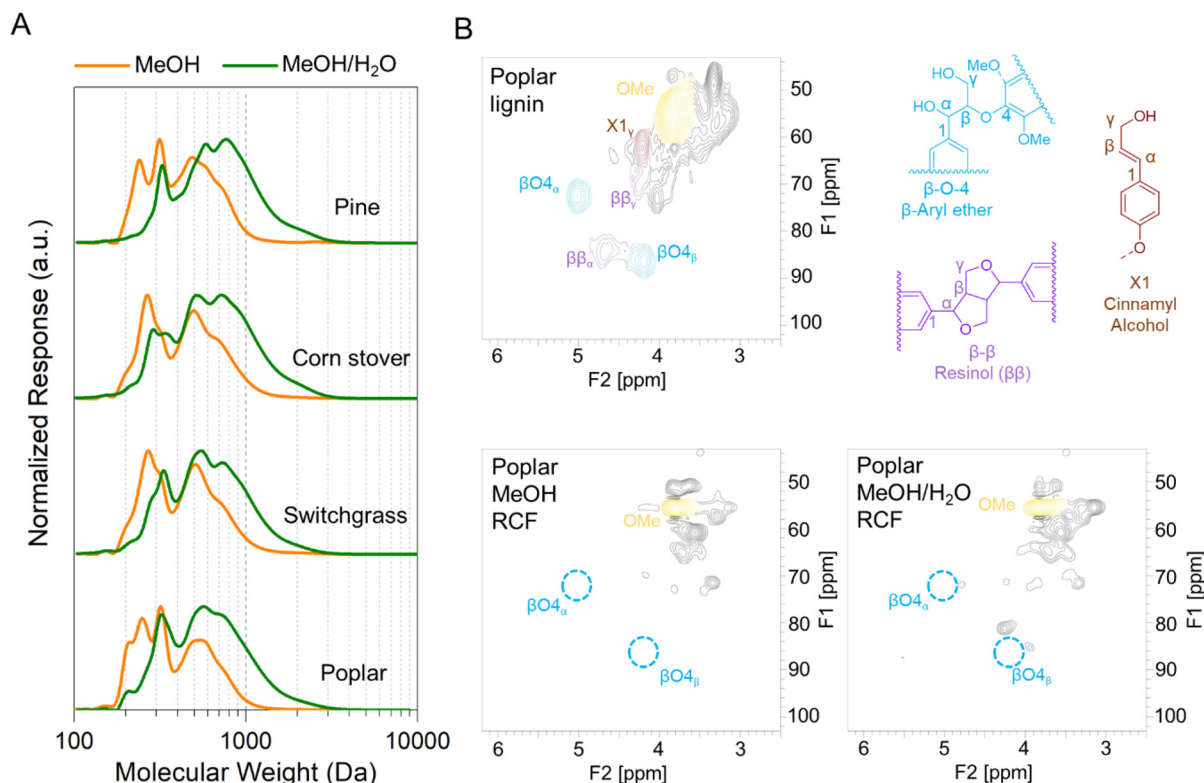


**Fig. 5** (A) GPC traces of lignin oil from FT-RCF with poplar, switchgrass, corn stover, and pine in methanol or methanol/water mixture. (B) NMR spectra of lignin before and after the catalysis step in RCF. Poplar lignin represents the extracted lignin through FT-solvolysis without the catalysis step. MeOH and MeOH/H<sub>2</sub>O are post FT-RCF (tandem solvolysis and catalysis) of poplar samples. The full spectra are presented in Fig. S10.†



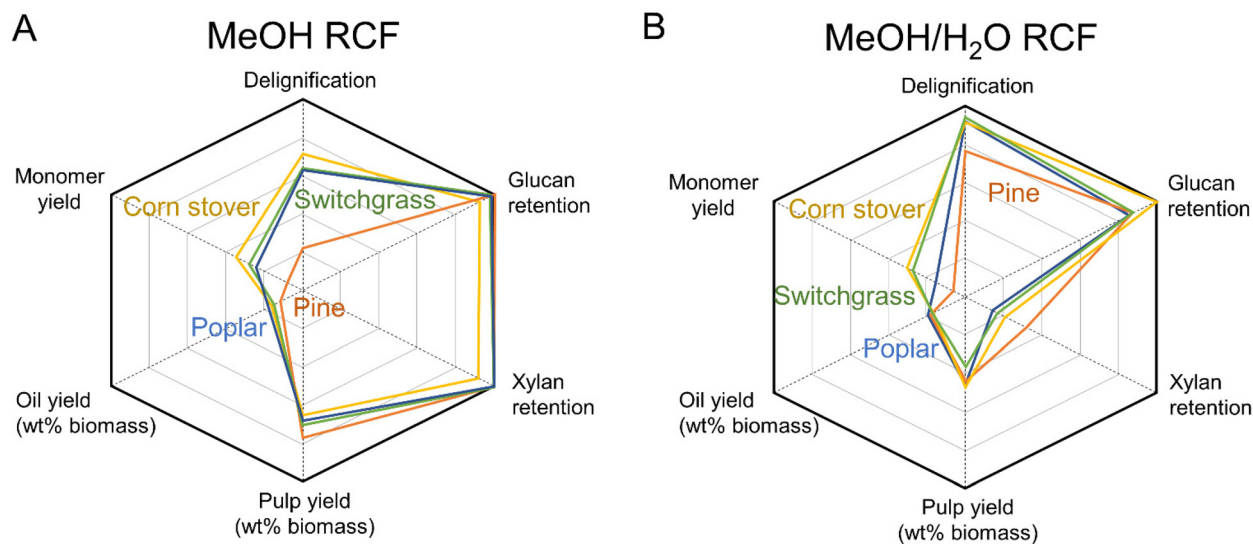


Fig. 6 FT-RCF performance over different feedstocks (A) in methanol and (B) in methanol/water mixture.

kages in the NMR spectrum rules out the possibility of ineffective lignin depolymerization due to water, and instead suggests condensation. We posited that condensation arose between the biomass bed and catalyst bed, wherein the extracted lignin remained at the reaction temperature before encountering the catalyst for stabilization. In the batch reaction, the extracted lignin could react with the catalyst immediately after extraction, thus achieving higher monomer yield ( $33.4 \pm 0.7\%$ ) and less condensation, evident by GPC traces (Fig. S6†).

The cumulative monomer yields for switchgrass and corn stover in methanol were  $27.0 \pm 1.4\%$  and  $35.8 \pm 1.6\%$ , respectively, close to the value observed in poplar FT-RCF ( $25.2 \pm 1.7$ ). As observed in the batch reactions, ethyl phenol, methyl-dihydrocoumarate, and methyl-dihydroferulate were the major products, as well as arylpropyl and arylpropanol monomers (Fig. 3). These monomers are consistent with the peaks at 200 and 270 Da in the GPC trace (Fig. 5A) and peaks in HSQC spectra (Fig. S11†). In methanol/water RCF, condensation and the resulting (1) lower portion of monomer peaks (Fig. 5A) and (2) lower yields of S/G-type monomers (Fig. 3) were also observed for switchgrass and corn stover. However, hydroxycinnamate-derived monomers were not reduced by adding water (Fig. 3). FT-RCF of pine showed cumulative monomer yields of  $6.5 \pm 0.1\%$  in methanol and  $6.3 \pm 0.5\%$  in methanol/water. It should be noted that theoretical maximum monomer yields depend on the abundance of  $\beta$ -ether units in lignin and the low monomer yields of pine RCF were due to the lower  $\beta$ -O-4 frequency of pine than for other feedstocks.<sup>50</sup>

## Discussion

The FT-RCF reaction and analysis of the obtained liquid and solid samples revealed the overall performance of RCF with different types of feedstocks in both the alcohol and alcohol/

water solvent systems. Fig. 6 and Table S4† summarize the FT-RCF process performance including delignification, monomer yield, glucan and xylan retention, and oil and pulp yields across all four feedstocks. Poplar, switchgrass, and corn stover exhibited similar delignification (64–71% in methanol and 92–95% in methanol/water), glucan retention (93–105% in methanol and 86–101% in methanol/water), and xylan retention (93–108% in methanol and 15–22% in methanol/water). These similarities across RCF performances with poplar, switchgrass, and corn stover suggest the potential as a feedstock-agnostic process.

Pine RCF with methanol exhibited a lower extent of lignin extraction (33%) than other feedstocks. The recalcitrant nature of pine resulted in the reduced efficiency of RCF with methanol, as observed in previous studies.<sup>31,51</sup> Despite the lower delignification extent, pine has a higher lignin content (34% of dried biomass) than other feedstocks (17–26%). As a result, pine RCF produced a similar yield of the isolated lignin oil on a dried biomass basis (12%), compared to values observed in RCF with other feedstocks (15–18%, Fig. 6A). It is worth noting that although switchgrass and corn stover have low lignin content (17–18%), the high content of extractives/acetates included in the isolated lignin oil resulted in a similar value of oil yield per dried biomass (Fig. 2A). In batch RCF with various biomass feedstocks in methanol, this study exhibited 14–17% lignin oil yields per biomass, which is in line with previous work, which ranged from 8–17% (Table S5†).

In methanol/water (Fig. 6B), delignification of pine RCF increased to 78%, close to the delignification values observed with hardwoods and herbaceous biomasses (92–95%). Samec *et al.* reported similar delignification values (84–94%) from RCF with 50:50 v/v ethanol/water across hardwoods (birch and poplar) and softwoods (spruce and pine), with low monomer yields (7–12%) obtained from softwoods (Table S5†).<sup>60</sup> The reduced gap in delignification values



between pine and other feedstocks, combined with high lignin content of pine, resulted in similar yields of the lignin oil (17–20%) regardless of feedstock. The oil yields in batch RCF in methanol/water in this study ranged 16–26%, which is in line with previous work in alcohol/water from 17–26% (Table S5†). Interestingly, GPC traces of the lignin oil from all tested feedstocks were similar for a given solvent system (Fig. 5A). In addition to the similarities in the yields and GPC traces of the lignin oil across feedstocks, the yield of pulp residue of each biomass did not vary significantly (65–77% from methanol RCF and 37–48% from methanol/water RCF). Thus, the similar yields and GPC traces of oil and pulp yields support the possibility of a feedstock-agnostic process with all types of biomass tested in this study.

The concept of feedstock-agnostic RCF could be made more tractable with breakthroughs in separation technology because each type of biomass has different monomer compositions (Fig. 1 and 3).<sup>61–65</sup> Pine RCF produced only G-type monomers with significantly lower yields, based on total lignin, under all tested reaction conditions relative to the RCF with other feedstocks. Conversely, RCF of poplar, switchgrass, and corn stover exhibited similar monomer yields, with hydroxycinnamate-derived monomers observed exclusively in RCF of herbaceous biomass, making different monomer distributions between poplar and herbaceous biomasses. A submitted paper from Ralph *et al.* describes in detail the impact of biomass type on the yield and distribution of phenolic monomers, distinguishing the monomers from the core lignin and from pendant units on the cell wall.<sup>66</sup> Batch RCF reactions with 16 different biomass feedstocks exhibit the monomer yields (based on Klason lignin) with the order of hardwood (43–55%) > herbaceous biomass (29–30%) > softwoods (15–16%).<sup>66</sup> Beyond separation approaches, methods for whole oil valorization, such as the recently demonstrated hydrodeoxygenation of whole RCF oil to produce jet-range fuels,<sup>59</sup> could also be a viable downstream method for processing lignin oils in a feedstock-agnostic context, which we will evaluate in future studies. Concerning catalyst stability, reversible (poisoning) and irreversible (sintering and leaching) deactivation was previously observed under RCF conditions.<sup>22</sup> In addition to a recent novel catalyst design for mitigation of the sintering problem during lignin hydrogenolysis,<sup>67</sup> further investigation of deactivation mechanisms and regeneration methods of RCF catalysts should be explored.

## Conclusions

In summary, we conducted batch and FT-RCF reactions with different types of biomass feedstock including poplar, switchgrass, corn stover, and pine using alcohol and alcohol/water solvent systems. In methanol, batch RCF of poplar, switchgrass, and corn stover at 230 °C produced similar yields of aromatic monomers (31–33%). The recalcitrant nature of pine resulted in lower lignin extraction extent and lower monomer yield (13%). Batch RCF with ethanol exhibited similar

monomer yields (27–31% for poplar, switchgrass, and corn stover and 11% for pine), compared to RCF in methanol. The use of water as a co-solvent significantly increased the lignin oil yield, and the overall monomer yields remained similar. Based on compositional analysis of the delignified pulp residue from FT-RCF, fractionation efficiency including delignification and glucan/xylan retention was similar across poplar, switchgrass, and corn stover. FT-RCF produced comparable monomer yields (25–36% in methanol and 15–32% in methanol/water) to batch RCF across hardwood and grasses and lower monomer yields (6–7%) of pine. Through batch and FT-RCF, herbaceous feedstocks produced S/G-type and hydroxycinnamate-derived monomers, whereas poplar included S/G-type monomers and pine yielded only G-type monomers. Despite the lower delignification and monomer yield of pine RCF, due to its higher lignin content the lignin oil yield on a biomass basis was similar to that in RCF of other hardwood and herbaceous feedstocks. These results suggest the industrial potential of RCF as a feedstock-agnostic process.

## Conflicts of interest

There are no conflicts to declare.

## Acknowledgements

This work was authored by the National Renewable Energy Laboratory, operated by the Alliance for Sustainable Energy, LLC, for the U.S. Department of Energy (DOE) under Contract No. DE-AC36-08GO28308. Funding was provided by the U.S. DOE Office of Energy Efficiency and Renewable Energy Bioenergy Technologies Office. We also acknowledge funding from ExxonMobil. The views expressed in the article do not necessarily represent the views of the DOE or the U.S. Government.

## References

- 1 T. L. Richard, *Science*, 2010, **329**, 793–796.
- 2 N. Sathitsuksanoh, Z. Zhu and Y. H. Zhang, *Bioresour. Technol.*, 2012, **117**, 228–233.
- 3 J. Rencoret, A. Gutierrez, L. Nieto, J. Jimenez-Barbero, C. B. Faulds, H. Kim, J. Ralph, A. T. Martinez and J. C. Del Rio, *Plant Physiol.*, 2011, **155**, 667–682.
- 4 A. Lourenço, J. Gominho, A. V. Marques and H. Pereira, *J. Wood Chem. Technol.*, 2013, **33**, 1–18.
- 5 V. Balan, L. D. C. Sousa, S. P. Chundawat, D. Marshall, L. N. Sharma, C. K. Chambliss and B. E. Dale, *Biotechnol. Prog.*, 2009, **25**, 365–375.
- 6 C. E. Wyman, B. E. Dale, R. T. Elander, M. Holtzapple, M. R. Ladisch, Y. Y. Lee, C. Mitchinson and J. N. Saddler, *Biotechnol. Prog.*, 2009, **25**, 333–339.



- 7 A. I. Osman, N. Mehta, A. M. Elgarahy, A. Al-Hinai, A. A. H. Al-Muhtaseb and D. W. Rooney, *Environ. Chem. Lett.*, 2021, **19**, 4075–4118.
- 8 J. Shi, V. S. Thompson, N. A. Yancey, V. Stavila, B. A. Simmons and S. Singh, *Biofuels*, 2014, **4**, 63–72.
- 9 C. Li, D. Tanjore, W. He, J. Wong, J. L. Gardner, V. S. Thompson, N. A. Yancey, K. L. Sale, B. A. Simmons and S. Singh, *BioEnergy Res.*, 2015, **8**, 982–991.
- 10 L. M. Hennequin, K. Polizzi, P. S. Fennell and J. P. Hallett, *RSC Adv.*, 2021, **11**, 18395–18403.
- 11 R. Rinaldi, R. Jastrzebski, M. T. Clough, J. Ralph, M. Kennema, P. C. Bruijninx and B. M. Weckhuysen, *Angew. Chem., Int. Ed.*, 2016, **55**, 8164–8215.
- 12 T. Renders, S. Van den Bosch, S. F. Koelewijn, W. Schutyser and B. F. Sels, *Energy Environ. Sci.*, 2017, **10**, 1551–1557.
- 13 W. Schutyser, T. Renders, S. Van den Bosch, S. F. Koelewijn, G. T. Beckham and B. F. Sels, *Chem. Soc. Rev.*, 2018, **47**, 852–908.
- 14 Z. Sun, B. Fridrich, A. de Santi, S. Elangovan and K. Barta, *Chem. Rev.*, 2018, **118**, 614–678.
- 15 T. Renders, G. Van den Bossche, T. Vangeel, K. Van Aelst and B. Sels, *Curr. Opin. Biotechnol.*, 2019, **56**, 193–201.
- 16 Y. M. Questell-Santiago, M. V. Galkin, K. Barta and J. S. Luterbacher, *Nat. Rev. Chem.*, 2020, **4**, 311–330.
- 17 M. M. Abu-Omar, K. Barta, G. T. Beckham, J. S. Luterbacher, J. Ralph, R. Rinaldi, Y. Román-Leshkov, J. S. M. Samec, B. F. Sels and F. Wang, *Energy Environ. Sci.*, 2021, **14**, 262–292.
- 18 E. M. Anderson, R. Katahira, M. Reed, M. G. Resch, E. M. Karp, G. T. Beckham and Y. Román-Leshkov, *ACS Sustainable Chem. Eng.*, 2016, **4**, 6940–6950.
- 19 D. Brandner, J. S. Kruger, N. E. Thornburg, G. G. Facas, J. K. Kenny, R. J. Dreiling, A. R. C. Morais, T. Renders, N. S. Cleveland, R. M. Happs, R. Katahira, T. Vinzant, D. G. Wilcox, Y. Román-Leshkov and G. T. Beckham, *Green Chem.*, 2021, **23**, 5437–5441.
- 20 T. Renders, E. Cooreman, S. Van den Bosch, W. Schutyser, S. F. Koelewijn, T. Vangeel, A. Deneyer, G. Van den Bossche, C. M. Courtin and B. F. Sels, *Green Chem.*, 2018, **20**, 4607–4619.
- 21 A. W. Bartling, M. L. Stone, R. J. Hanes, A. Bhatt, Y. Zhang, M. J. Bidy, R. Davis, J. S. Kruger, N. E. Thornburg, J. S. Luterbacher, R. Rinaldi, J. S. M. Samec, B. F. Sels, Y. Román-Leshkov and G. T. Beckham, *Energy Environ. Sci.*, 2021, **14**, 4147–4168.
- 22 E. M. Anderson, M. L. Stone, R. Katahira, M. Reed, G. T. Beckham and Y. Román-Leshkov, *Joule*, 2017, **1**, 613–622.
- 23 I. Kumaniaev, E. Subbotina, J. Sävmarker, M. Larhed, M. V. Galkin and J. S. M. Samec, *Green Chem.*, 2017, **19**, 5767–5771.
- 24 S. Van den Bosch, T. Renders, S. Kennis, S. F. Koelewijn, G. Van den Bossche, T. Vangeel, A. Deneyer, D. Depuydt, C. M. Courtin, J. M. Thevelein, W. Schutyser and B. F. Sels, *Green Chem.*, 2017, **19**, 3313–3326.
- 25 E. M. Anderson, M. L. Stone, M. J. Hülsey, G. T. Beckham and Y. Román-Leshkov, *ACS Sustainable Chem. Eng.*, 2018, **6**, 7951–7959.
- 26 T. Ren, S. You, Z. Zhang, Y. Wang, W. Qi, R. Su and Z. He, *Green Chem.*, 2021, **23**, 1648–1657.
- 27 D. Di Francesco, K. R. Baddigam, S. Muangmeesri and J. S. M. Samec, *Green Chem.*, 2021, **23**, 9401–9405.
- 28 J. H. Jang, D. G. Brandner, R. J. Dreiling, A. J. Ringsby, J. R. Bussard, L. M. Stanley, R. M. Happs, A. S. Kovali, J. I. Cutler, T. Renders, J. R. Bielenberg, Y. Román-Leshkov and G. T. Beckham, *Joule*, 2022, **6**, 1859–1875.
- 29 E. Subbotina, A. Velty, J. S. M. Samec and A. Corma, *ChemSusChem*, 2020, **13**, 4528–4536.
- 30 J. K. Kenny, D. G. Brandner, S. R. Neefe, W. E. Michener, Y. Román-Leshkov, G. T. Beckham and J. W. Medlin, *React. Chem. Eng.*, 2022, **7**, 2527–2533.
- 31 Y. Liao, S. F. Koelewijn, G. V. D. Bossche, J. V. Aelst, S. V. D. Bosch, T. Renders, K. Navare, T. Nicolai, K. V. Aelst, M. Maesen, H. Matsushima, J. M. Thevelein, K. V. Acker, B. Lagrain, D. Verboekend and B. F. Sels, *Science*, 2020, **367**, 1385–1390.
- 32 I. Graça, R. T. Woodward, M. Kennema and R. Rinaldi, *ACS Sustainable Chem. Eng.*, 2018, **6**, 13408–13419.
- 33 J. Park, A. Riaz, D. Verma, H. J. Lee, H. M. Woo and J. Kim, *ChemSusChem*, 2019, **12**, 1743–1762.
- 34 J. Chen, F. Lu, X. Si, X. Nie, J. Chen, R. Lu and J. Xu, *ChemSusChem*, 2016, **9**, 3353–3360.
- 35 M. V. Galkin and J. S. Samec, *ChemSusChem*, 2014, **7**, 2154–2158.
- 36 Z. Cao, M. Dierks, M. T. Clough, I. B. Daltro de Castro and R. Rinaldi, *Joule*, 2018, **2**, 1118–1133.
- 37 E. O. Ebikade, N. Samulewicz, S. Xuan, J. D. Sheehan, C. Wu and D. G. Vlachos, *Green Chem.*, 2020, **22**, 7435–7447.
- 38 H. Luo, I. M. Klein, Y. Jiang, H. Zhu, B. Liu, H. I. Kenttämä and M. M. Abu-Omar, *ACS Sustainable Chem. Eng.*, 2016, **4**, 2316–2322.
- 39 R. N. Nishide, J. H. Truong and M. M. Abu-Omar, *ACS Omega*, 2021, **6**, 8142–8150.
- 40 F. Brienza, K. Van Aelst, F. Devred, D. Magnin, B. F. Sels, P. A. Gerin, I. Cybulska and D. P. Debecker, *ACS Sustainable Chem. Eng.*, 2022, **10**, 11130–11142.
- 41 N. E. Thornburg, M. B. Pecha, D. G. Brandner, M. L. Reed, J. V. Vermaas, W. E. Michener, R. Katahira, T. B. Vinzant, T. D. Foust, B. S. Donohoe, Y. Roman-Leshkov, P. N. Ciesielski and G. T. Beckham, *ChemSusChem*, 2020, **13**, 4495–4509.
- 42 A. Sluiter, R. Ruiz, C. Scarlata, J. Sluiter and D. Templeton, *Determination of extractives in biomass*, Report NREL/TP-510-42619, National Renewable Energy Laboratory, Golden, Colorado, USA, 2005.
- 43 A. Sluiter, B. Hames, R. Ruiz, C. Scarlata, J. Sluiter, D. Templeton and D. Crocker, *Determination of structural carbohydrates and lignin in biomass*, Report NREL/TP-510-



- 42618, National Renewable Energy Laboratory, Golden, Colorado, USA, 2008.
- 44 A. Sluiter, B. Hames, R. Ruiz, C. Scarlata, J. Sluiter and D. Templeton, *Determination of ash in biomass*, Report NREL/TP-510-42622, National Renewable Energy Laboratory, Golden, Colorado, USA, 2008.
  - 45 S. D. Mansfield, H. Kim, F. Lu and J. Ralph, *Nat. Protoc.*, 2012, **7**, 1579–1589.
  - 46 W. Schutyser, S. Van den Bosch, T. Renders, T. De Boe, S. F. Koelewijn, A. Dewaele, T. Ennaert, O. Verkinderen, B. Goderis, C. M. Courtin and B. F. Sels, *Green Chem.*, 2015, **17**, 5035–5045.
  - 47 T. Renders, S. Van den Bosch, T. Vangeel, T. Ennaert, S.-F. Koelewijn, G. Van den Bossche, C. M. Courtin, W. Schutyser and B. F. Sels, *ACS Sustainable Chem. Eng.*, 2016, **4**, 6894–6904.
  - 48 H. Luo and M. M. Abu-Omar, *Green Chem.*, 2018, **20**, 745–753.
  - 49 A. Gupta and J. P. Verma, *Renewable Sustainable Energy Rev.*, 2015, **41**, 550–567.
  - 50 M. V. Galkin, A. T. Smit, E. Subbotina, K. A. Artemenko, J. Bergquist, W. J. Huijgen and J. S. Samec, *ChemSusChem*, 2016, **9**, 3280–3287.
  - 51 S. Van den Bosch, W. Schutyser, R. Vanholme, T. Driessen, S. F. Koelewijn, T. Renders, B. De Meester, W. J. J. Huijgen, W. Dehaen, C. M. Courtin, B. Lagrain, W. Boerjan and B. F. Sels, *Energy Environ. Sci.*, 2015, **8**, 1748–1763.
  - 52 S. Van den Bosch, W. Schutyser, S. F. Koelewijn, T. Renders, C. M. Courtin and B. F. Sels, *ChemComm*, 2015, **51**, 13158–13161.
  - 53 J. Ralph, *Phytochem. Rev.*, 2009, **9**, 65–83.
  - 54 S. Su, L. P. Xiao, X. Chen, S. Wang, X. H. Chen, Y. Guo and S. R. Zhai, *ChemSusChem*, 2022, **15**, e202200365.
  - 55 E. M. Anderson, M. L. Stone, R. Katahira, M. Reed, W. Muchero, K. J. Ramirez, G. T. Beckham and Y. Román-Leshkov, *Nat. Commun.*, 2019, **10**, 2033.
  - 56 I. Kumaniaev, E. Subbotina, M. V. Galkin, P. Srifa, S. Monti, I. Mongkolpichayarak, D. N. Tungasmita and J. S. M. Samec, *Pure Appl. Chem.*, 2020, **92**, 631–639.
  - 57 A. Kramarenko, D. Etit, G. Laudadio and F. N. D'Angelo, *ChemSusChem*, 2021, **14**, 3838–3849.
  - 58 X. Liu, F. P. Bouxin, J. Fan, V. L. Budarin, C. Hu and J. H. Clark, *ChemSusChem*, 2020, **13**, 4296–4317.
  - 59 M. L. Stone, M. S. Webber, W. P. Mounfield, D. C. Bell, E. Christensen, A. R. C. Morais, Y. Li, E. M. Anderson, J. S. Heyne, G. T. Beckham and Y. Román-Leshkov, *Joule*, 2022, **6**, 2324–2337.
  - 60 M. V. Galkin, A. T. Smit, E. Subbotina, K. A. Artemenko, J. Bergquist, W. J. Huijgen and J. S. M. Samec, *ChemSusChem*, 2016, **9**, 3280–3287.
  - 61 Z. Sultan, I. Graca, Y. Li, S. Lima, L. G. Peeva, D. Kim, M. A. Ebrahim, R. Rinaldi and A. G. Livingston, *ChemSusChem*, 2019, **12**, 1203–1212.
  - 62 E. Cooreman, T. Vangeel, K. Van Aelst, J. Van Aelst, J. Lauwaert, J. W. Thybaut, S. Van den Bosch and B. F. Sels, *Ind. Eng. Chem. Res.*, 2020, **59**, 17035–17045.
  - 63 Z. Sun, J. Cheng, D. Wang, T. Q. Yuan, G. Song and K. Barta, *ChemSusChem*, 2020, **13**, 5199–5212.
  - 64 S. S. Wong, R. Shu, J. Zhang, H. Liu and N. Yan, *Chem. Soc. Rev.*, 2020, **49**, 5510–5560.
  - 65 T. Croes, A. Dutta, R. De Bie, K. Van Aelst, B. Sels and B. Van der Bruggen, *Chem. Eng. J.*, 2023, **452**, 139418.
  - 66 M. Chen, Y. Li, F. Lu, J. S. Luterbacher and J. Ralph, Manuscript submitted for publication.
  - 67 F. Talebkeikhah, S. Sun and J. S. Luterbacher, *Adv. Energy Mater.*, 2023, **13**, 2203377.

